Angewandte Chemie
Eine Zeitschrift der Gesellschaft Deutscher Chemiker

Supporting Information

69451 Weinheim, Germany

NMR Spectroscopy of Soluble Protein Complexes at One Mega-Dalton and Beyond**

*Andi Mainz, Tomasz L. Religa, Remco Sprangers, Rasmus Linser, Lewis E. Kay, and Bernd Reif**

anie_201301215_sm_miscellaneous_information.pdf

Supporting Information for the Manuscript:

Affiliations:

[1]Munich Center for Integrated Protein Science (CIPS-M) at Department Chemie, Technische Universität Muenchen (TUM), Lichtenbergstr. 4, 85747 Garching, Germany.

[2]Helmholtz-Zentrum Muenchen (HMGU), Deutsches Forschungszentrum für Gesundheit und Umwelt, Ingolstädter Landstr. 1, 85764 Neuherberg, Germany.

[3]Leibniz-Institut für Molekulare Pharmakologie (FMP), Robert-Roessle-Str. 10, 13125 Berlin, Germany.

[4]University of Toronto, Department of Medical Genetics and Microbiology, 1 King's College Circle, Ontario, Canada M5S 1A8.

[5]Program in Molecular Structure and Function, Hospital for Sick Children, 555 University Avenue, Toronto, Ontario, Canada M5G 1X8.

[6]Max Planck-Institute for Developmental Biology, Spemannstr. 35–39, 72076 Tuebingen, Germany.

[7]Harvard Medical School, Department of Biological Chemistry and Molecular Pharmacology, 240 Longwood Ave, Boston, MA 02115.

[8]School of Chemistry, UNSW, Sydney 2052, Australia.

*Correspondence to: reif@tum.de

Table of contents:

Materials and Methods:

Preparation of the proteasome subunits

The proteasome α- (Uniprot accession code P25156) and β-subunits (Uniprot accession code P28061) from *Thermoplasma acidophilum* as well as the 11S activator from *Trypanosoma brucei* (PA26, Uniprot accession code Q9U8G2) were separately expressed, purified and subsequently assembled as reported elsewhere.[1,2] Only the α-subunit was isotopically enriched with ^{13}C and ^{15}N. For ^{13}C-detected experiments, the α- and β-subunits were recombinantly expressed in 100% H_2O minimal medium, yielding fully protonated samples. Protein perdeuteration for ^{1}H-detected experiments was achieved by expressing all components (α, β and 11S) in minimal medium with 100% D_2O (Sigma Aldrich). For sparse protonation of water-exchangeable groups, the deuterated α- and β-subunits were were denatured in 50 mM potassium phosphate, 7 M guanidine hydrochloride, 1 mM DTT, pH 7.5, 0.03% sodium azide, 20% H_2O and 80% D_2O for 10 minutes at 80 °C.[1,2] Renaturation was performed by rapid refolding into 50 mM potassium phosphate, 100 mM sodium chloride, 1 mM DTT, pH 7.5, 0.03% sodium azide, 20% H_2O and 80% D_2O. The native 11S activator was buffer-exchanged several times to assure the desired protonation level of 20%. For 11S-$\alpha_7\beta_7\beta_7\alpha_7$-11S samples, the 11S activator was added to the $\alpha_7\beta_7\beta_7\alpha_7$ core particle with 1.5 molar excess. The U-[^{2}D], Ileδ1-[$^{13}CHD_2$], Leu, Val-[$^{13}CHD_2$,$^{13}CD_3$]-labeled $\alpha_7\alpha_7$ sample was prepared as described previously.[1,2]

NMR sample preparation

The FROSTY samples were prepared as shown previously.[3] Briefly, the proteasome samples were concentrated using ultrafiltration devices for volumes up to 4 mL and 0.4 mL (Millipore). Glycerol was added to the samples during the concentration procedure with final contents of 30-40% *v*/*v*. The protein concentration was carefully quantified by measuring the absorption at a wavelength of 280 nm with a Nanodrop ND-1000 instrument (PeqLab), and by using molar extinction coefficients of 16,390 ($\alpha_7\alpha_7$), 29,800 ($\alpha_7\beta_7\beta_7\alpha_7$) and 51,230 $M^{-1}\,cm^{-1}$ (11S-$\alpha_7\beta_7\beta_7\alpha_7$-11S), respectively. The obtained viscous, non-turbid protein solutions were filled directly into 4 mm or 3.2 mm MAS rotors (Bruker Biospin) with sample volumes of 40 µL and 20 µL, respectively.

NMR spectroscopy and data analysis

The ^{13}C-detected MAS NMR experiments were performed using a wide-bore 16.4 T NMR spectrometer (Bruker Biospin) equipped with a standard 4 mm triple resonance MAS probe. 1D cross polarization (CP)[4] and 2D proton-driven spin diffusion (PDSD)[5] spectra were obtained for the fully protonated 360 kDa $\alpha_7\alpha_7$ (3.5 mM monomeric α-subunit) and the 670 kDa $\alpha_7\beta_7\beta_7\alpha_7$ complex (2.3 mM monomeric α-subunit) in phosphate buffer containing 40% *v*/*v* glycerol. The

experiments were performed under identical conditions, i.e. at an effective sample temperature of –10 °C and with 12 kHz MAS. The samples were spun for several hours prior to the NMR experiments in order to fully sediment the protein complexes. A recycle delay of 2.5 s was used. ^{1}H heteronuclear decoupling during evolution and mixing periods was achieved by applying a two-pulse phase modulated (TPPM)[6] scheme with radio frequency (rf) fields of 77 kHz.

Magnetization transfer between ^{1}H and ^{13}C was achieved via CP. The rf field strengths were matched according to the $n = -1$ Hartmann-Hahn condition[7] and considering the linear ramp (75-100%) on the ^{13}C channel (64 kHz (^{1}H), 45 kHz (^{13}C)). CP durations were optimized individually to account for the differential dynamics of the two assemblies. Contact pulses of 250 µs ($\alpha_7\alpha_7$) and 800 µs ($\alpha_7\beta_7\beta_7\alpha_7$), respectively, were found to give optimal signal-to-noise ratios for the aliphatic region. However, the short CP duration for $\alpha_7\alpha_7$ led to non-efficient build-up of C' signal intensities.

The 2D PDSD spectra were recorded with a mixing time of 50 ms. The PDSD spectrum of $\alpha_7\alpha_7$ was recorded with twice the number of scans (256) in order to compensate for the lower sensitivity. The acquisition times were 5 ms (410 t_1 increments at a sweep width of 40000 Hz) and 12 ms for the indirect and the direct ^{13}C dimensions, respectively. The time domains of both dimensions were multiplied with a squared sine-bell function (shift of the bell by 60°) and zero-filled to obtain a matrix of 2048×1024 data points after Fourier transformation.

2D ^{1}H-^{15}N correlation spectra were acquired at a magnetic field strength of 14.1 T and a MAS frequency of 22 kHz. The effective sample temperature was initially set to 0 °C for all proteasome assemblies due to sensitivity issues. Additional spectra of 11S-$\alpha_7\beta_7\beta_7\alpha_7$-11S were recorded at temperatures of 20, 30 and 40 °C. In general, low temperatures yield higher signal intensities in FROSTY experiments utilizing dipole-dipole couplings (through-space) (Figure S4B). The content of glycerol and the choice of temperature are thus important parameters for FROSTY experiments, which must be adapted individually to the respective biological system.

The employed concentrations of the NMR-active α-subunit amounted to 3.3 mM ($\alpha_7\alpha_7$), 1.9 mM ($\alpha_7\beta_7\beta_7\alpha_7$) and 3.0 mM (11S-$\alpha_7\beta_7\beta_7\alpha_7$-11S), respectively, in phosphate buffer containing 20% H_2O, 80% D_2O and 30% deuterated glycerol. Proton densities of this order have been reported to provide an optimal compromise in terms of sensitivity and resolution for the spinning speeds used in this study.[8] The samples were spun for several hours prior to the NMR experiments to assure sedimentation equilibration.

Recycle delays were shortened by Cu^{II}-mediated paramagnetic relaxation enhancement.[9,10] A stock solution of 400 mM Cu^{II}-EDTA (Sigma Aldrich) in phosphate buffer containing 20% H_2O, 80% D_2O and 30% perdeuterated glycerol (Sigma Aldrich) was added to the proteasome samples to a final concentration of the paramagnetic agent of 60 mM. In order to optimize the recycle delay, ^{1}H longitudinal relaxation times T_1 were determined for the bulk amide region. The proteasome assemblies in the absence of Cu^{II}-EDTA revealed ^{1}H T_1 values on the order of 2 s. The addition of 60 mM Cu^{II}-EDTA resulted in short ^{1}H T_1 of approximately 100-200 ms, thus reducing the measurement time by a factor of >10. The recycle delay was set to two times the measured ^{1}H T_1 value to ensure comparable experimental conditions for the different proteasome samples. The recycle delay was on the order of 0.4 s (0 °C) and 0.2 s (40 °C), respectively.

Cross polarization from $^{1}H_N$ to $^{15}N_H$ was performed according to the $n = -1$ Hartmann-Hahn condition with rf field strengths in the range of 60 kHz (^{1}H) and 35 kHz (^{15}N), respectively. A linear ramp (75-100%) on the ^{15}N channel was used. CP durations of 0.5 ms were used for all proteasome complexes. Heteronuclear decoupling of ^{1}H and ^{15}N was achieved with rf field strengths of 4 kHz and 2 kHz (Waltz-16), respectively. *J*-decoupling of ^{13}C during ^{15}N evolution was achieved with a composite ^{13}C π-pulse. Due to the high content of water in FROSTY samples, suppression of the water resonance was achieved by implementing a pulse train of 4×15 ms with a rf field strength of 4-10 kHz and alternating phase during longitudinal ^{15}N magnetization.[11,12] The 2D ^{1}H-^{15}N (and 3D hCXhNH experiments adapted from[13,14]) were designed in a constant-time fashion here to ensure reproducible dephasing of the water resonance as well as to yield optimal signal-to-noise ratios. Transmitters were placed at 4.7 ppm (^{1}H) and 119 ppm (^{15}N), respectively. The acquisition times in the ^{1}H and ^{15}N dimension amounted to 30 ms and 58 ms (256 t_1 increments at a sweep width of 2190 Hz), respectively. The presented 2D ^{1}H-^{15}N CP correlation spectra were acquired by accumulating 512 spectra per increment according to an experimental time of about 14 h. 2D spectra of 11S-$\alpha_7\beta_7\beta_7\alpha_7$-11S were obtainable in about 2 h with sufficient signal-to-noise ratio. The time domains of both dimensions were multiplied with a squared sine-bell function (shift of the bell by 60°) and zero-filled to finally obtain a matrix of 2048×1024 data points after Fourier transformation. The INEPT- and TROSY-based ^{1}H-^{15}N correlation experiments were performed as previously reported.[15] All other acquisition and processing parameters were similar to those given for the CP-based variant (see above).

3D hCXhNH spectra of 11S-$\alpha_7\beta_7\beta_7\alpha_7$-11S were acquired at a magnetic field strength of 14.1 T, a MAS rate of 22 kHz and an effective temperature of 30 °C. The long-range $^{1}H_N$-^{13}C CP field strengths were optimized in order to achieve selective magnetization transfer to either the C' or Cα/Cβ nuclei. A duration of 1.6 ms was used for the long-range CP. ^{13}C transmitter offsets and sweep widths were set to 174 ppm and 2940 Hz (hCOhNH), and to 44 ppm and 10420 Hz (hCAhNH), respectively. No *J*-decoupling of $^{13}C'$ and $^{13}C\alpha$ nuclei was implemented during ^{13}C evolution due to significant loss in sensitivity. The acquisition times of the 3D hCOhNH spectrum amounted to 30 ms, 16 ms (64 t_2 increments) and 11 ms (64 t_1 increments) for ^{1}H, ^{15}N and ^{13}C, respectively. The corresponding values for the 3D hCAhNH spectrum were 30 ms, 16 ms (64 t_2 increments) and 5.4 ms (112 t_1 increments), respectively. Both spectra were recorded with 128 transients per increment and a recycle delay of 0.2 s giving rise to experimental times of approximately 5 d (hCAhNH) and 3 d (hCOhNH), respectively. The spectra were processed with a squared sine-bell function (shift of the bell by 90°) in all dimensions and zero-filling to a final data matrix of 2048×256×256 points. Approximately 20 amide correlations were not assigned due to missing correlations in the ^{13}C dimension, missing sequential information and/or due to larger deviations from the solution-state chemical shifts of α_7. The 3D hCAhNH and hCOhNH experiments were similarly performed at 0 °C and yielded resonance assignment for 73 residues.

The 2D ^{1}H-^{13}C correlation spectrum of U-[^{2}D], Ileδ1-[$^{13}CHD_2$], Leu, Val-[$^{13}CHD_2$, $^{13}CD_3$] $\alpha_7\alpha_7$ was recorded without Cu^{II}-EDTA (recycle delay of 2 s). The spectrum was recorded at an effective temperature of 0 °C, with 20 kHz MAS and at a magnetic field strength of 16.4 T. The $\alpha_7\alpha_7$ complex was employed at a monomer concentration of 3.5 mM in phosphate buffer containing 20% H_2O, 80% D_2O and 40% perdeuterated glycerol. During the CP of 2 ms duration, rf fields of 76 kHz (^{1}H) and 49 kHz (^{13}C) were applied in consideration of the linear

ramp on ^{13}C (75-100%). Decoupling of ^{2}H during ^{13}C evolution was achieved with an rf field strength of 4 kHz (Waltz-16). The spectrum was recorded with 128 scans and with acquisition times of 40 ms and 21 ms (190 t_1 increments at a ^{13}C sweep width of 4500 Hz) in the ^{1}H and ^{13}C dimensions, respectively. The ^{13}C transmitter was placed at 19 ppm. The spectrum was processed with a squared sine-bell function (shift of the bell by 60°) in both dimensions and zero-filling to a final data matrix of 2048×512 points.

Data acquisition and processing was done using TopSpin 2.0 (Bruker Biospin), further data analysis and resonance assignments were performed using the software Sparky.[16] ^{13}C chemical shift indices[17] and secondary structure elements were derived using the CcpNmr Analysis software.[18] Theoretical rotational correlation times τ_c were estimated with the program Hydro-NMR.[19] PDB entries 1PMA[20] and 1YA7[21] were used for the estimations. The calculations were run for a temperature of 30 °C and the corresponding viscosity of water (0.798×10^{-2} Poise). Molecular structures were visualized with PyMol (Delano Scientific LLC). To illustrate the size and shape of the $\alpha_7\alpha_7$ complex, the $\alpha_7\beta_7$ double ring of the full proteasome $\alpha_7\beta_7\beta_7\alpha_7$ structure is depicted in Figure 1 and Figure 3.

Sedimentation calculations

The protein fraction f sedimented by MAS under the employed experimental conditions was estimated according to Bertini *et al.*[22]:

$$f = \frac{c_{\mathrm{limit}}\pi(r^2 - a^2)}{c_0\pi r^2}$$

where r is the internal radius of the MAS rotor (1.5 mm for 4 mm rotor and 1.2 mm for 3.2 mm rotor), c_0 is the employed concentration of the protein complex and c_{limit} denotes the maximum protein concentration, which is derived from the maximum protein density (1,430 kg m^{-3} times a packing coefficient for spherical particles of 0.74) divided by the protein molecular weight M_{w}. The parameter a corresponds to the distance from the rotor axis at which the maximum protein concentration c_{limit} is reached and is given by:

$$a = \left[r^2\left(1 - \frac{c_0}{c_{\mathrm{limit}}}\right) + \frac{2RT}{M_w(1 - \rho_{solv}/\rho_{prot})\omega_R{}^2} \right]^{1/2}$$

with ω_{R} being the angular rotor speed, ρ_{prot} denoting the protein density, ρ_{solv} representing the density of the solvent at the employed temperature T and with R being the ideal gas constant. Solvent densities ρ_{solv} of 1,111 kg m^{-3} at –10 °C (40% *v/v* glycerol in water, ^{13}C-detected experiments) and 1,085 kg m^{-3} at 0 °C (30% *v/v* glycerol in water, ^{1}H-^{15}N correlation experiments) were used for the calculations. For the ^{1}H-^{15}N correlation experiments (3.2 mm rotor, 22 kHz MAS, 0 °C, 30% *v/v* glycerol) the following protein sediment fractions f are calculated: 97.7% ($\alpha_7\alpha_7$), 98.8% ($\alpha_7\beta_7\beta_7\alpha_7$) and 99.7% (11S-$\alpha_7\beta_7\beta_7\alpha_7$-11S), respectively. The corresponding values for the ^{13}C-detected experiments (4 mm rotor, 12 kHz MAS, –10 °C, 40% *v/v* glycerol) amount to 95.1% ($\alpha_7\alpha_7$) and 97.8% ($\alpha_7\beta_7\beta_7\alpha_7$), respectively. For comparison, the calculations for the single α-subunit (26 kDa, 3.5 mM) under the same experimental conditions yield theoretical fractions f of approximately 69% (3.2 mm rotor) and 31% (4 mm rotor), respectively. This shows that much higher spinning rates are required to access smaller proteins.

Supporting Figures S1-S5:

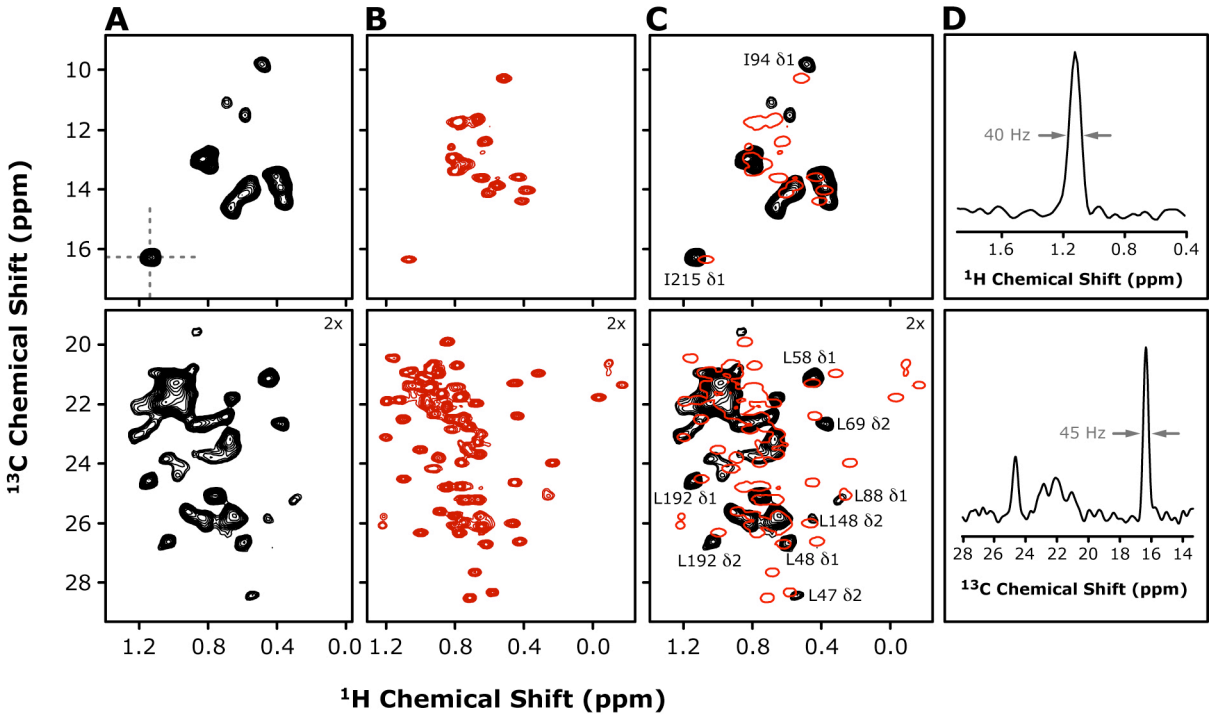

Figure S1. Detection of methyl groups in the 360 kDa half-proteasome $\alpha_7\alpha_7$. ***(A)*** Sections of the 2D ^{1}H-^{13}C CP spectrum of U-[^{2}D], Ileδ1-[$^{13}CHD_2$], Leu, Val-[$^{13}CHD_2$,$^{13}CD_3$] $\alpha_7\alpha_7$ (black) showing methyl resonances of isoleucines-δ1 (top), and leucines and valines (bottom), respectively. The solution-state HMQC TROSY spectrum of $\alpha_7\alpha_7$ (red)[1] is shown in ***(B)*** and superimposed with the 2D ^{1}H-^{13}C CP spectrum in ***(C)***. In all spectra, cross peaks of Leu and Val are drawn at lower contour level (2x) for better visualization. Resonances which can clearly be identified from solution-state NMR assignments are labeled. ***(D)*** 1D projections at ^{1}H and ^{13}C chemical shifts of the I215-δ1 cross peak in the ^{1}H-^{13}C CP spectrum (see (A)). The corresponding line widths at half-height are indicated. In light of the improved resolution and sensitivity in ^{1}H-^{15}N correlation experiments, we also expect a gain in spectral quality for the larger $\alpha_7\beta_7\beta_7\alpha_7$ and 11S-$\alpha_7\beta_7\beta_7\alpha_7$-11S complexes. For the FROSTY sample, $\alpha_7\alpha_7$ was employed at a concentration of 92 mg mL^{-1} (~3.5 mM) in phosphate buffer containing 20% H_2O, 80% D_2O and 40% perdeuterated glycerol. The spectrum was recorded at an effective temperature of 0 °C, with 20 kHz MAS and at 16.4 T, whereas the solution-state TROSY spectrum was acquired at 50 °C and 18.8 T.[1]

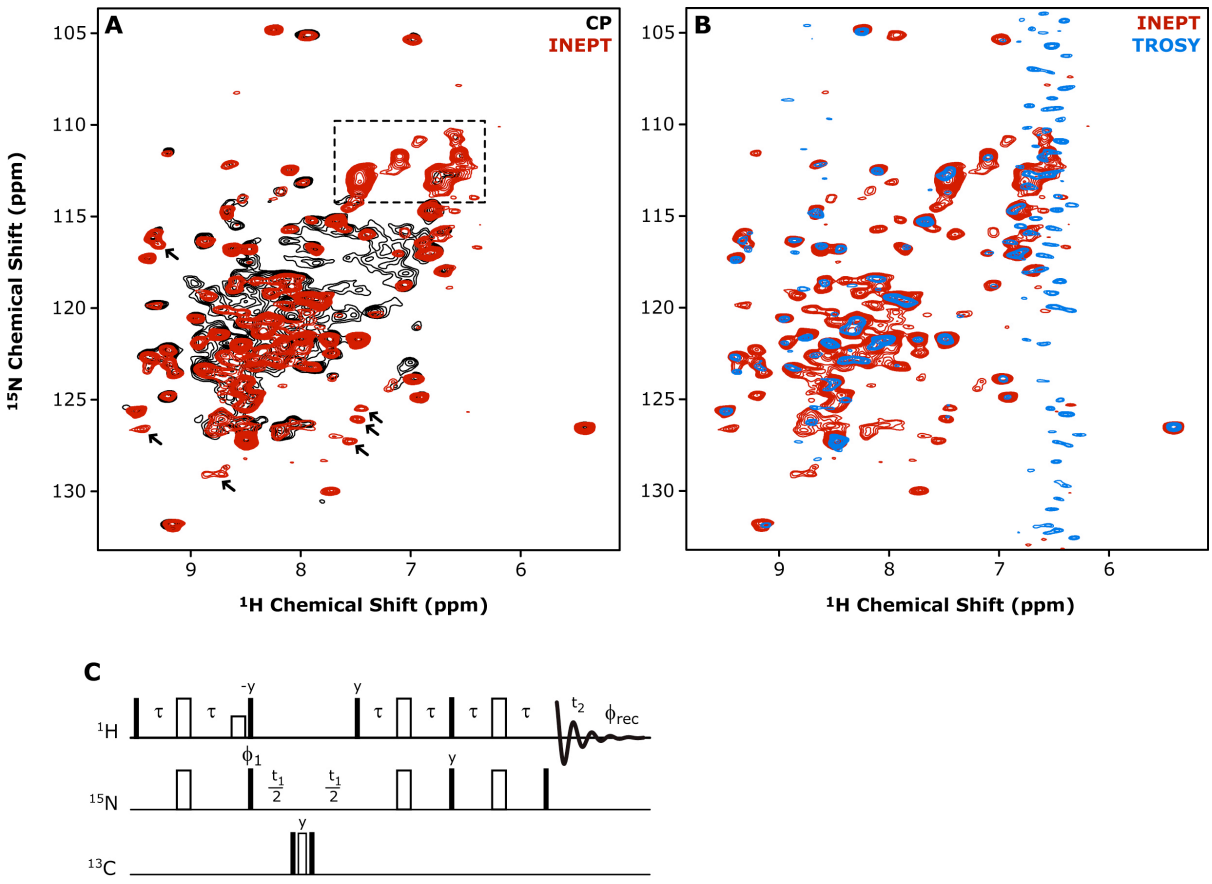

Figure S2. Comparison of experiments using dipolar (through-space) and scalar couplings (through-bond) for magnetization transfer. ***(A)*** 2D ^{1}H-^{15}N correlation spectra of 11S-$\alpha_7\beta_7\beta_7\alpha_7$-11S employing dipolar-based CP (black) and scalar-based INEPT transfer steps (red). Arrows highlight resonances, which are exclusively observed in the INEPT version. The dashed box indicates side-chain amides of Gln and Asn residues. ***(B)*** The 2D ^{1}H-^{15}N correlation spectrum of 11S-$\alpha_7\beta_7\beta_7\alpha_7$-11S using INEPT (red) is superimposed with the corresponding TROSY spectrum (blue). TROSY has been shown to provide advantages for certain kinds of scalar transfers when fast relaxation occurs due to motionally induced differential relaxation.[15] No additional resonances were observed in the TROSY ^{1}H-^{15}N correlation experiment. All spectra were recorded at 20 °C. ***(C)*** Pulse scheme for TROSY experiments as shown in (B). Phases ϕ_1 and ϕ_{rec} include phase-sensitive incrementation and spin-state selection by 90 degree shifts as described in the original application.[23] Water suppression by only 1ms spin lock pulse in the initial INEPT (open rectangle with reduced height) leads to significant remaining water artifacts (visible in the figure at 6.5 ppm ^{1}H chemical shift). The application of field gradients, as routinely done in solution-state NMR for efficient water suppression, is also expected to improve the suppression of water artifacts and thus to yield higher sensitivity.

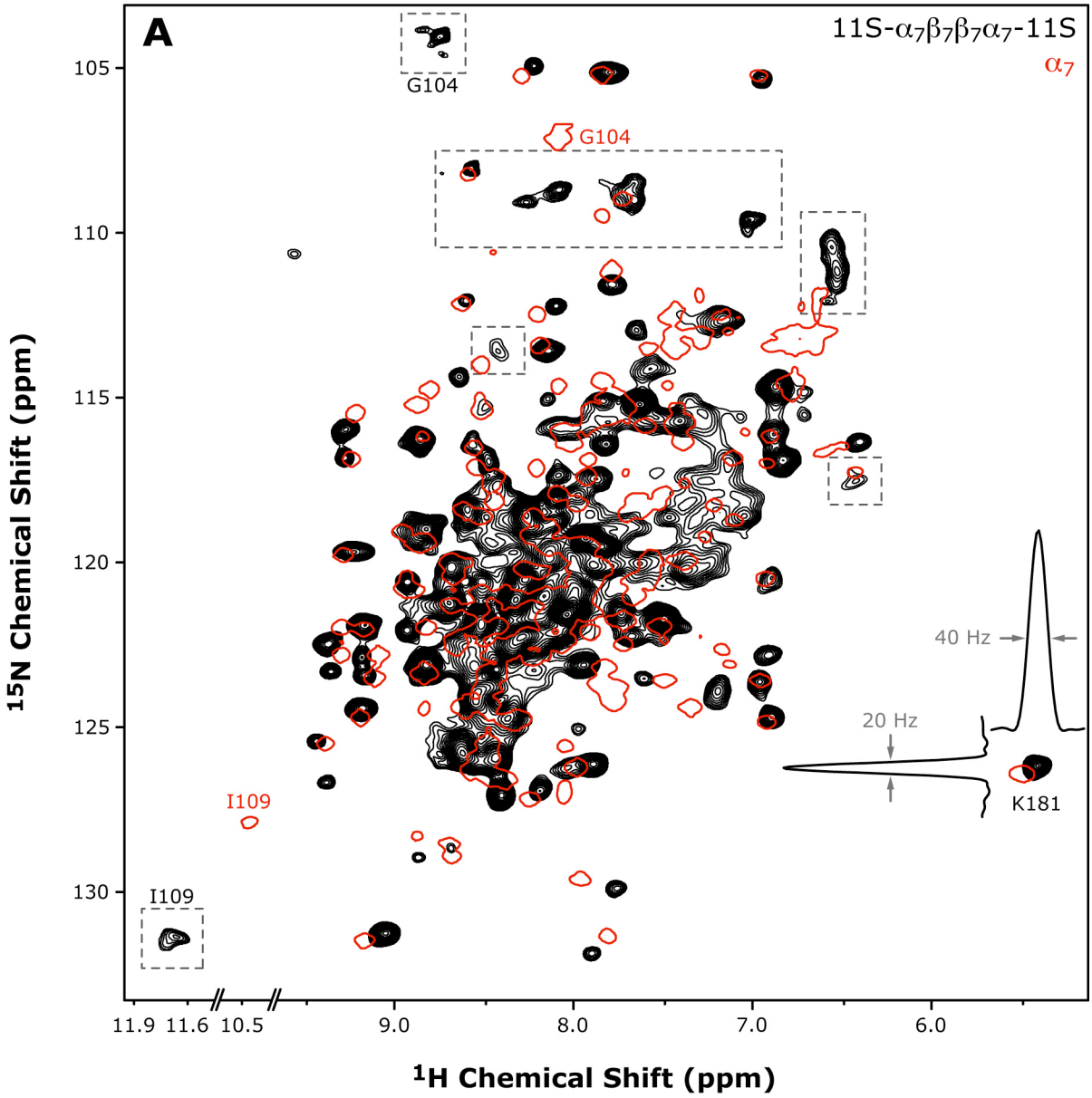
A
11S-α7β7β7α7-11S
α7
G104
G104
I109
I109
40 Hz
20 Hz
K181
105
110
115
120
125
130
11.9
11.6
10.5
9.0
8.0
7.0
6.0
15N Chemical Shift (ppm)
1H Chemical Shift (ppm)

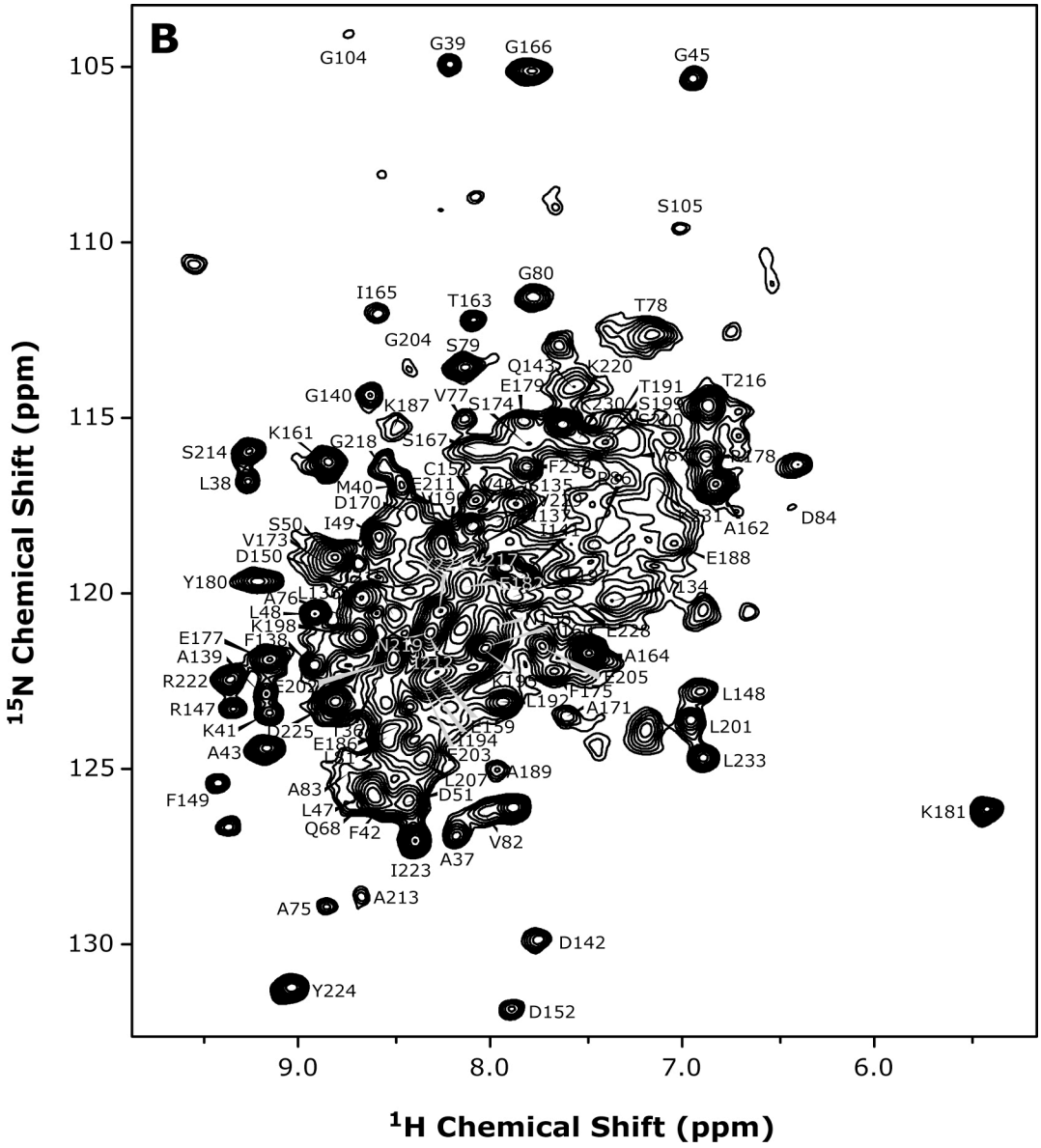

Figure S3. Backbone resonances of the proteasome α-subunit within the 1.1 MDa 11S-$\alpha_7\beta_7\beta_7\alpha_7$-11S complex observed by FROSTY MAS NMR. **(*A*)** The CP-based ^{1}H-^{15}N correlation spectrum of the full proteasome in complex with the 11S activator is shown in black. Note that resonances in dashed boxes are drawn at lower contour levels (2.3x) for better comparison. 1D projections and the corresponding line widths at half-height for ^{1}H and ^{15}N are illustrated for K181. The spectrum is superimposed with the solution-state ^{1}H-^{15}N TROSY spectrum of the 180 kDa heptameric α_7 construct (red)[2]. The strongly perturbed resonances of G104 and I109, which are located at the binding interface between the α- and β-subunit, are labeled. The FROSTY spectrum was recorded at an effective temperature of 30 °C and with22 kHz MAS, whereas the solution-state TROSY spectrum of α_7 was acquired at 50 °C.[2] **(*B*)** 2D ^{1}H-^{15}N correlation spectrum with resonance assignments (drawn using the same contour level for the whole spectrum).

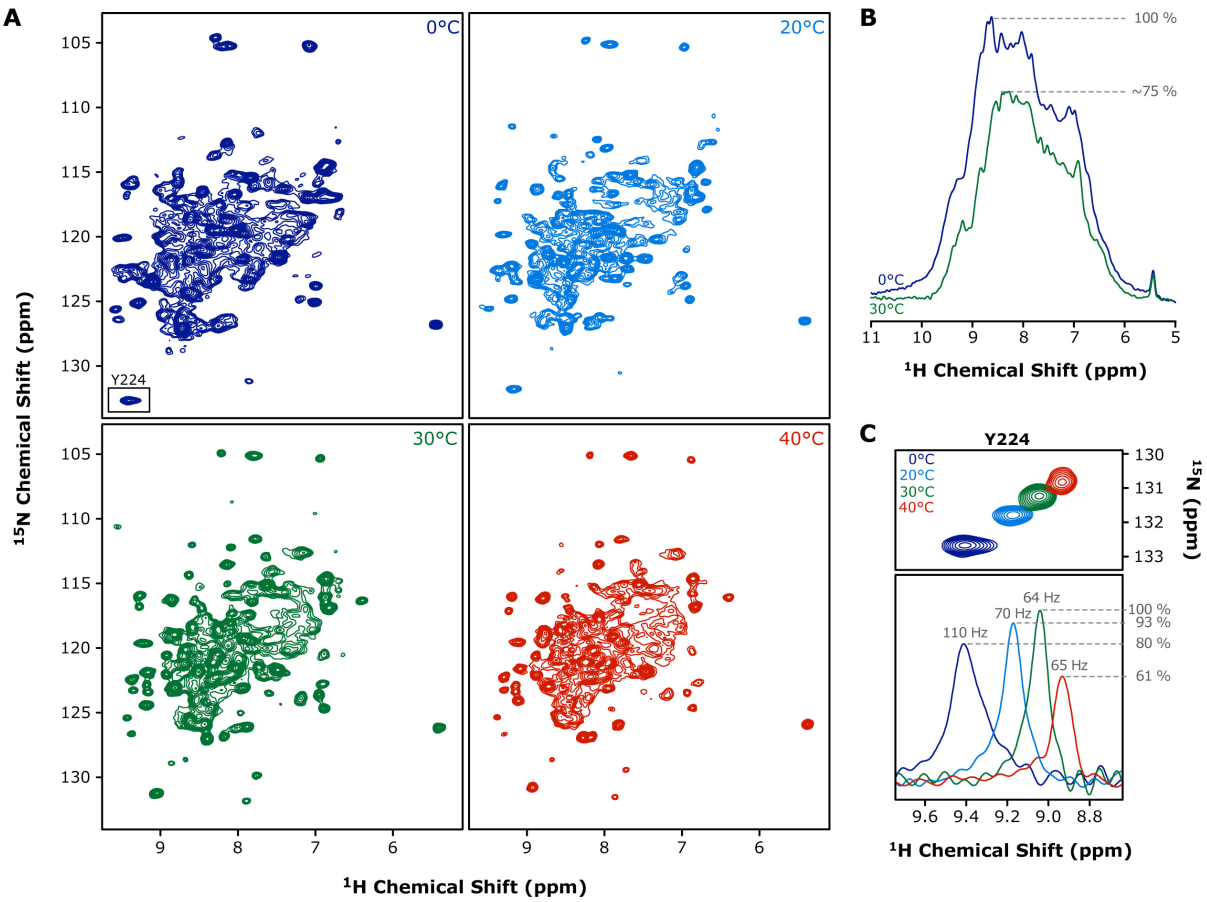

Figure S4. Temperature dependence of proton-detected FROSTY experiments. ***(A)*** 2D ^{1}H-^{15}N correlation spectra of 11S-$\alpha_7\beta_7\beta_7\alpha_7$-11S at 0 °C (dark blue), 20 °C (light blue), 30 °C (green) and 40 °C (red), respectively. The low-field resonance of I109 is omitted. ***(B)*** Sensitivity loss for the bulk amide region with increasing temperature. 1D CP spectra of 11S-$\alpha_7\beta_7\beta_7\alpha_7$-11S are shown for the temperatures 0 °C (dark blue) and 30 °C (green), both at which assignment experiments were performed. ***(C)*** The resonance of Y224 is enlarged from the spectra shown in (A) to exemplarily illustrate the line-narrowing observed for several resonances due to conformational averaging at higher temperatures. 1D projections extracted at the ^{15}N chemical shift of Y224 are depicted on the bottom. ^{1}H line widths at half-height and relative signal intensities are given for each temperature step.

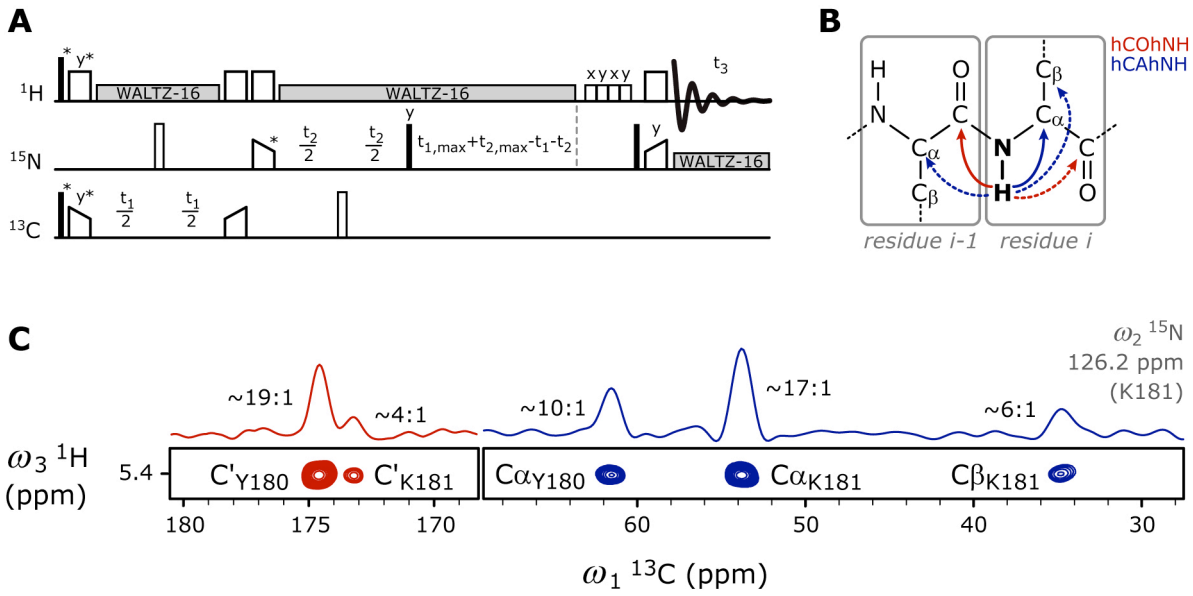

Figure S5. The hCXhNH experiment as developed from[13,14]. ***(A)*** Pulse scheme: After excitation of both ^{1}H and ^{13}C, magnetization is transferred from amide protons to dipolar-coupled carbons employing a long-range CP step with durations of approximately 2 ms. Asterisks denote pulse phases incremented during TPPI. The experiment was designed as „constant-time“ in this work to optimize water suppression. ***(B)*** Observed correlations: Each amide proton is dipolar-coupled to carbon atoms of its own residue *i* (intra-residual) and to carbon nuclei of the preceding residue *i*–1 (inter-residual). The CP contact pulse is optimized to achieve magnetization transfer either to carbonyl (hCOhNH, red arrows) *or* to aliphatic nuclei (hCAhNH, blue arrows). More and less intense correlations are drawn using solid and dashed lines, respectively. The experiment also yields weak correlations to the Cβ of residue *i*. In principle, more side-chain information may be obtained in the future by including a ^{13}C-^{13}C mixing sequence in the pulse scheme shown in (A). This will further aid the assignment process. ***(C)*** Representative 2D ^{1}H-^{13}C strips from the 3D hCOhNH (red) and hCAhNH (blue) spectra extracted at the ^{15}N chemical shift of K181. The corresponding 1D slice is shown above to illustrate the quality of the data. Peaks are labeled with assignments and signal-to-noise ratios, respectively.

Supporting References:

[1] R. Sprangers, L. E. Kay, *Nature* **2007**, *445*, 618–622.

[2] R. Sprangers, X. Li, X. Mao, J. L. Rubinstein, A. D. Schimmer, L. E. Kay, *Biochemistry* **2008**, *47*, 6727–6734.

[3] A. Mainz, S. Jehle, B. J. van Rossum, H. Oschkinat, B. Reif, *J. Am. Chem. Soc.* **2009**, *131*, 15968–15969.

[4] A. Pines, M. G. Gibby, J. S. Waugh, *J. Chem. Phys.* **1973**, *59*, 569–590.

[5] N. M. Szeverenyi, M. J. Sullivan, G. E. Maciel, *J. Magn. Reson.* **1982**, *47*, 462–475.

[6] A. E. Bennett, C. M. Rienstra, M. Auger, K. V. Lakshmi, R. G. Griffin, *J. Chem. Phys.* **1995**, *103*, 6951–6958.

[7] S. R. Hartmann, E. L. Hahn, *Phys. Rev.* **1962**, *128*, 2042–2053.

[8] U. Akbey, S. Lange, W. Trent Franks, R. Linser, K. Rehbein, A. Diehl, B.-J. van Rossum, B. Reif, H. Oschkinat, *J. Biomol. NMR* **2010**, *46*, 67–73.

[9] N. P. Wickramasinghe, M. Kotecha, A. Samoson, J. Past, Y. Ishii, *J. Magn. Reson.* **2007**, *184*, 350–356.

[10] R. Linser, V. Chevelkov, A. Diehl, B. Reif, *J. Magn. Reson.* **2007**, *189*, 209–216.

[11] E. K. Paulson, C. R. Morcombe, V. Gaponenko, B. Dancheck, R. A. Byrd, K. W. Zilm, *J. Am. Chem. Soc.* **2003**, *125*, 15831–15836.

[12] D. H. Zhou, C. M. Rienstra, *J. Magn. Reson.* **2008**, *192*, 167–172.

[13] R. Linser, *J. Biomol. NMR* **2012**, *52*, 151–158.

[14] R. Linser, *J. Biomol. NMR* **2011**, *51*, 221–226.

[15] R. Linser, U. Fink, B. Reif, *J. Am. Chem. Soc.* **2010**, *132*, 8891–8893.

[16] T. D. Goddard, D. G. Kneller, SPARKY 3, University of California, San Fransisco

[17] D. S. Wishart, B. D. Sykes, *J. Biomol. NMR* **1994**, *4*, 171–180.

[18] W. F. Vranken, W. Boucher, T. J. Stevens, R. H. Fogh, A. Pajon, M. Llinas, E. L. Ulrich, J. L. Markley, J. Ionides, E. D. Laue, *Proteins* **2005**, *59*, 687–696.

[19] J. García de la Torre, M. L. Huertas, B. Carrasco, *J. Magn. Reson.* **2000**, *147*, 138–146.

[20] J. Löwe, D. Stock, B. Jap, P. Zwickl, W. Baumeister, R. Huber, *Science* **1995**, *268*, 533–539.

[21] A. Förster, E. I. Masters, F. G. Whitby, H. Robinson, C. P. Hill, *Mol. Cell* **2005**, *18*, 589–599.

[22] I. Bertini, C. Luchinat, G. Parigi, E. Ravera, B. Reif, P. Turano, *Proc. Natl. Acad. Sci. U.S.A.* **2011**, *108*, 10396–10399.

[23] K. Pervushin, R. Riek, G. Wider, K. Wüthrich, *Proc. Natl. Acad. Sci. U.S.A.* **1997**, *94*, 12366–12371.